Journal of Power Sources 242 (2013) 621–626

Contents lists available at SciVerse ScienceDirect

Journal of Power Sources

journal homepage: www.elsevier.com/locate/jpowsour

Short communication

Hydrogen generation from borohydride hydrolysis on surface-alloyed Ni foam

Z.P. Li [a,*], S.L. Ma [a], G.R. Li [a], B.H. Liu [b]

[a] Department of Chemical and Biological Engineering, Zhejiang University, Hangzhou 310027, People's Republic of China
[b] Department of Materials Science and Engineering, Zhejiang University, Hangzhou 310027, People's Republic of China

HIGHLIGHTS

- Porous Ni-based catalysts for borohydride hydrolysis are prepared by surface alloying in Ni foam.
- Raney Ni foam exhibits higher catalytic activity than Mg_2Ni formed on Ni foam struts.
- Falling film H_2-generation demonstrates high H_2 generation rate and quick response.

GRAPHICAL ABSTRACT

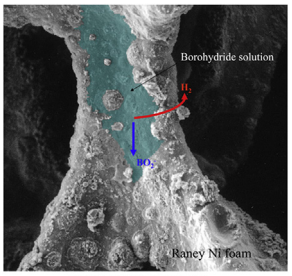

falling film H_2-generation

ARTICLE INFO

Article history:
Received 7 March 2013
Received in revised form
5 May 2013
Accepted 21 May 2013
Available online 5 June 2013

Keywords:
Borohydride hydrolysis
Hydrogen generation
Catalyst
Ni foam
Surface alloying
Falling film hydrogen generation

ABSTRACT

This work explores the use of falling film technology to generate hydrogen from BH_4^- hydrolysis reaction. A technique to create catalytic sites on Ni foam struts by surface alloying is also developed. Mg–Ni and Al–Ni intermetallic compounds (catalyst precursor) are formed when Ni foams loaded with Mg and Al powders are heated to 600 °C under N_2 atmosphere, respectively. The catalytic sites of Mg_2Ni and Raney Ni are formed on Ni foam struts after treating surface-alloyed Ni foams with an alkaline BH_4^- solution. Raney Ni on Ni foam struts (Raney Ni foam) has higher catalytic activity than Mg_2Ni on Ni foam struts. The Raney Ni foam reaction plate in falling film reactor demonstrates high catalytic activity and quick response to fuel feed in H_2 generation.

1. Introduction

Hydrogen is a potential and economical clean energy carrier stored in molecular (pressurized vessels, liquefied H_2 tanks), atomic (metal hydrides), or hydride forms (protide compounds). Hydrogen storage techniques that are related to liquid-phase chemical H storage materials, such as aqueous $NaBH_4$, H_3NBH_3, N_2H_4, $N_2H_4BH_3$, and HCO_2H, have attracted considerable attention [1]. The generation of H_2 from catalytic BH_4^- hydrolysis is a convenient way of supplying H_2 to on-board fuel cells [2–4] because of the following advantages: $NaBH_4$ solutions are nonflammable; reaction products (i.e., $NaBO_2$) are environmentally benign and recyclable; H_2 generation rates are easily controlled. The theoretical H amount released is 10.8 wt.% through $NaBH_4$ hydrolysis reaction, and half of the H originates from H_2O [5].

* Corresponding author. Tel./fax: +86 571 87953149.
E-mail address: zhoupengli@zju.edu.cn (Z.P. Li).

0378-7753/$ – see front matter © 2013 Elsevier B.V. All rights reserved.
http://dx.doi.org/10.1016/j.jpowsour.2013.05.103

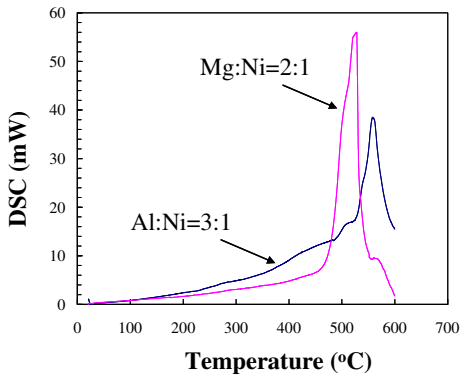

Fig. 1. Differential scanning calorimetry analysis of Ni foams loaded with Mg and Al powders, respectively. Heating rate: 5 °C min^{-1}.

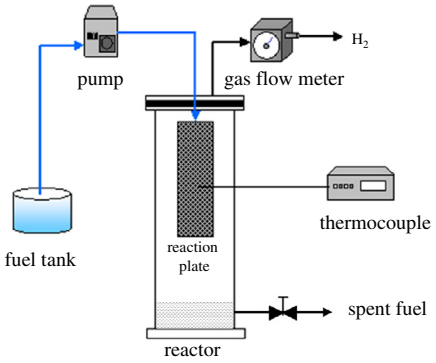

Fig. 2. Diagram of the falling film reactor for $NaBH_4$ hydrolysis.

H_2 generation from BH_4^- hydrolysis depends on the applied catalyst, reactant (BH_4^-) and product (BO_2^-) concentrations [6,7]. Mg and Al form alloys with Ni. Raney Ni is prepared by leaching Al from $NiAl_3$ and Ni_2Al_3 in a hot alkaline solution. Ni and Mg_2Ni are excellent catalysts in BH_4^- hydrolysis reaction [8–11]. However, catalyst erosion significantly deteriorates catalyst durability. Several catalyst support technologies have been developed by using ion exchange resin [12], γ-Al_2O_3 [13], TiO_2 [14], solid–acid sulphated zirconia [15,16], and SiO_2 [17] as support materials. The use of sponge materials for catalyst support effectively decreases catalyst erosion by decreasing the flow resistance of H_2 stream. Moreover, loading Ni or Co catalyst into Ni foam by chemical reduction produces highly active catalysts [18,19].

Catalysts are conventionally placed in a BH_4^- solution to catalyze BH_4^- hydrolysis reaction. Numerous H_2 bubbles evolve from the alkaline BH_4^- solution in this approach; the H_2 bubbles carry some liquid to form alkaline mist and thus decrease H purity [20]. Moreover, supplying H_2 on-demand is impractical because the applied catalyst cannot rapidly establish contact to and separation from the BH_4^- solution.

The falling film technique has been widely used in unit operations such as evaporation, crystallization, and microreaction. The process fluid involved in evaporation, crystallization, or reaction flows downwards as a continuous film because of gravity. Falling film microreactors offer many advantages over conventional batch reactors including improved reaction speed and conversion rate, safety, reliability, scalability, on-site/on-demand production, and ease of process control. H_2 generation from BH_4^- solutions is similar to evaporation. However, the design of the catalyst plate in H_2 generation is different from the design of the evaporation plate. This difference in design is one of the key issues in developing a falling film microreactor for H_2 generation.

This study aimed to develop a reliable on-demand hydrogen supply system to explore the use of falling film technology in generating H_2 from BH_4^- hydrolysis reaction catalyzed by a catalyst sheet. The anti-erosion ability of supported catalysts depends on the binding situation between the catalyst and its support. The creation of catalyst from a support forms a stronger bond between the catalyst and its support than a catalyst loaded to its support (conventional method). A porous catalyst preparation method was used to prevent catalyst erosion from the catalyst support by using surface alloying based on Ni foam. To strengthen the bond between the catalyst and its support, this work created Ni clusters from catalyst support (Ni foam) by treating the surface of the Ni foam that is alloyed with Mg and Al. Surface alloying effects were investigated by characterization and the kinetic study of H_2 generation. Factors influencing H_2 generation such as fuel concentration and fuel feed rate were investigated based on porous catalyst development.

Table 1
Specific surface area of Ni foam before and after surface alloying and activation.

	Ni foam	Mg-alloyed Ni foam	HF-treated Mg-alloyed Ni foam	Raney Ni foam
Specific surface area (m^2 g^{-1})	0.32	5.51	11.10	21.22

2. Experimental

2.1. Catalyst preparation

Mg and Al powder pastes were prepared by adding 10 g of Mg and Al powders (purity: 99.9%, <25 μm) to 50 mL of methylcellulose solution (2 wt.%) and stirred for 20 min at room temperature, respectively. Ni foam (WF10002D with 95% porosity and 1.7 mm thickness; Shanghai Winfay New Material Co., Ltd., China) loaded with metal powders was obtained after drying. The Ni foams were

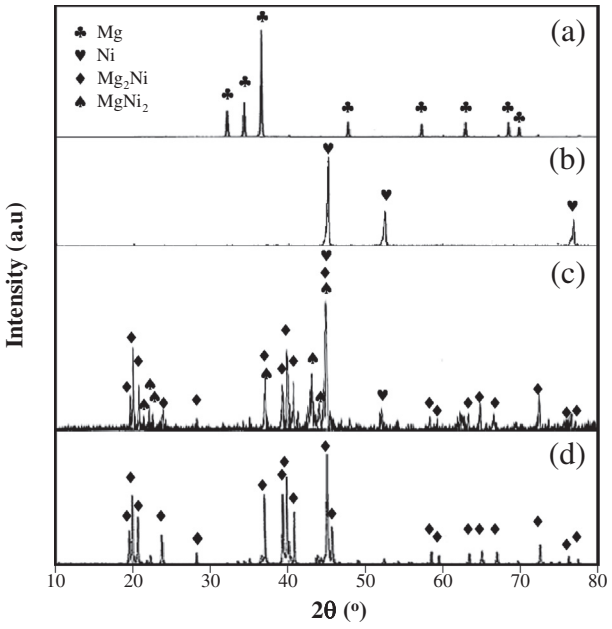

Fig. 3. X-ray diffraction patterns of (a) Mg powder, (b) Ni foam, (c) Mg-alloyed Ni foam and (d) removed substance from Mg-alloyed Ni foam after alkaline borohydride solution treatment.

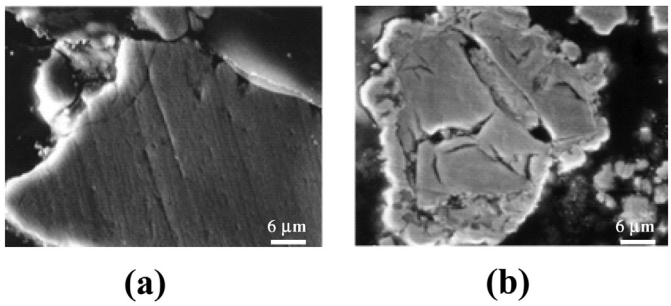

Fig. 4. Cross-sections of Mg_2Ni (a) before and (b) after alkaline borohydride solution treatment.

pasted with the Mg and Al powder pastes by using the atomic ratio of Mg:Ni = 2:1 and Al:Ni = 3:1, respectively. Based on the differential scanning calorimetry measurement of the pressed powder mixture, Mg–Ni and Al–Ni alloying occur around 480 °C (Fig. 1). To ascertain the formation of Mg–Ni and Al–Ni alloys (catalyst precursor), the surface alloying of Ni foam was conducted at 600 °C under N_2 atmosphere at a heating rate of 5 °C min^{-1}.

Surface-alloyed Ni foam was obtained after heating the Mg- or Al-loaded Ni foam at 600 °C for 30 min. The foam was then cooled to room temperature. Catalysts were activated by dipping the surface-alloyed Ni foam into an alkaline BH_4^- solution (containing 15 wt.% of $NaBH_4$ and 10 wt.% of NaOH) for 60 min at 30 °C. Loosely embedded pack materials were removed by the H_2 bubbles generated from BH_4^- hydrolysis. These catalysts were stored in an alkaline solution containing 10 wt.% of NaOH. Extreme caution must be exercised while handling these inflammable catalysts. The specific surface area of these catalysts was determined by the Brunauer–Emmett–Teller (BET) method by using Flow Sorb II 2300 (Micromeritics®). The sample was placed in a test cell and dried in a vacuum for 12 h after washing with de-ionized water several times at room temperature. The test cell was sealed after being charged with N_2 for BET measurement. The specific surface area values of the synthesized catalysts are listed in Table 1.

2.2. Physical characterization

The catalyst sample was mounted into a special resin and polished with diamond oil slurry (0.1 μm) to determine the cross-section composition profiles of the catalysts. The distribution of elements was identified by electron probe micro-analysis (EPMA) by using the Shimadzu EPMA-8705 (Shimadzu, Japan) at 20 kV and 0.1 mA. The microstructure and cross section of the synthesized catalysts were characterized by X-ray diffraction (XRD) by using a RINT 1000 diffractometer with Cu Kα radiation (λ = 1.5406 Å) and scanning electron microscopy (SEM attached to EPMA at 15 kV and 0.1 nA), respectively.

2.3. H_2 evolution

A piece of surface-alloyed Ni foam was used as the reaction plate instead of a multi-channel architecture used in conventional

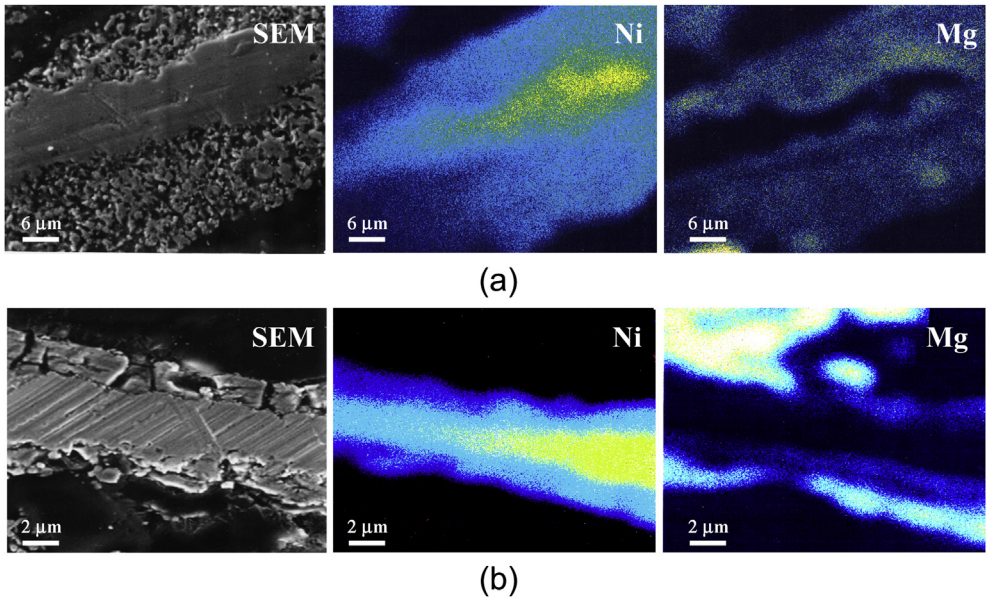

Fig. 5. Cross-section and element distribution of the Mg-alloyed Ni foam (a) before and (b) after alkaline borohydride solution treatment.

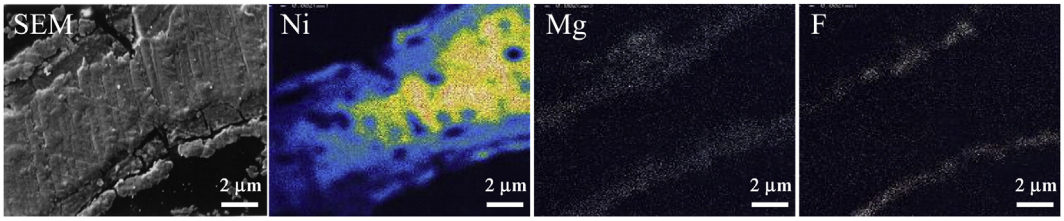

Fig. 6. Cross-section and element distribution of HF-treated Mg-alloyed Ni foam.

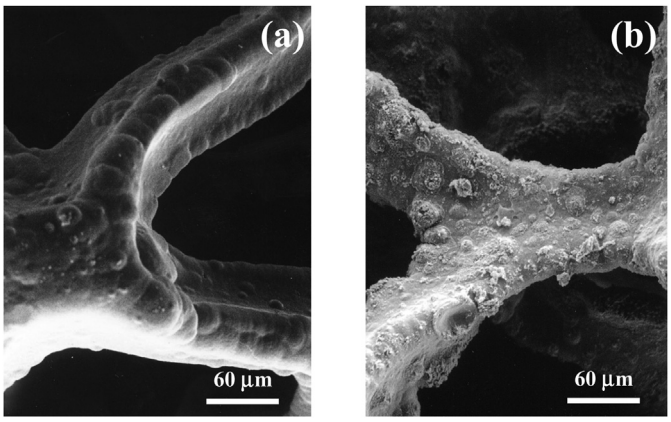

Fig. 7. Morphologies of (a) Ni foam and (b) Raney Ni foam.

falling film microreactors. A diagram of the falling film reactor for BH_4^- hydrolysis is illustrated in Fig. 2. The alkaline $NaBH_4$ solution, which is controlled by a peristaltic pump, flows from the top of the porous reaction plate at various feed rates. H_2 volume was measured by using a gas flow meter connected to a computer (for recording) and then converted to normal volume based on gas temperature. A thermocouple was placed in the reaction plate to monitor the temperature during BH_4^- hydrolysis.

3. Results and discussion

3.1. Physical characterization

Fig. 3(c) shows the XRD pattern of Mg-alloyed Ni foam after the alkaline BH_4^- solution treatment. Mg_2Ni, $MgNi_2$, and Ni are retained in the catalyst after the calcination of Mg-loaded Ni foam at 600 °C for 30 min. The XRD pattern of the removed substance from Mg-alloyed Ni foam after the alkaline BH_4^- solution treatment is shown in Fig. 3(d). The results indicate that the alkaline

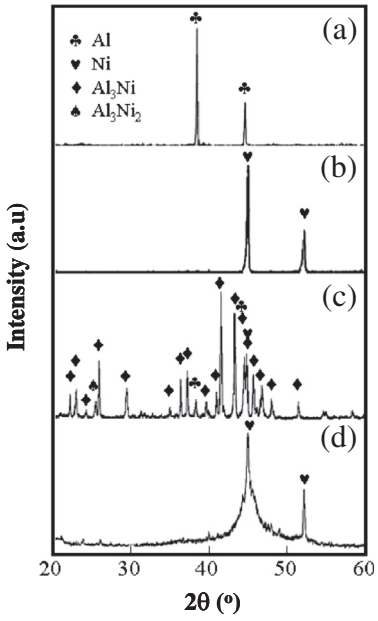

Fig. 8. X-ray diffraction patterns of (a) Al powder, (b) Ni foam, and Al-alloyed Ni foam (c) before and (d) after alkaline borohydride solution treatment.

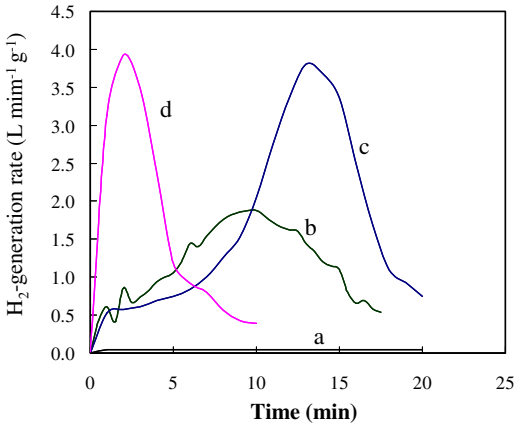

Fig. 9. H_2-generation rates from borohydride hydrolysis catalyzed by (a) bare Ni foam, (b) Mg-alloyed Ni foam, (c) HF-treated Mg-alloyed Ni foam and (d) Raney Ni foam in a batch reactor at 25 °C. Fuel: 30 mL (15 wt.% of $NaBH_4$ and 10 wt.% of NaOH).

BH_4^- solution treatment removes some Mg_2Ni particles from Ni foam struts.

The cross sections of Mg_2Ni particles before and after the alkaline BH_4^- solution treatment are shown in Fig. 4. Numerous cracks are created in the Mg_2Ni particle after the alkaline BH_4^- solution treatment because of the H_2 uptake of Mg_2Ni. Fig. 5 shows the cross section and element distribution of Mg-alloyed Ni foam before and after the alkaline BH_4^- solution treatment. The alkaline BH_4^- solution treatment removes Mg_2Ni alloy particles that are loosely formed on the Ni foam struts. Based on the Ni and Mg distributions shown in Fig. 5(b), Mg_2Ni (light color, outer layer) and $MgNi_2$ (dark color, inner layer) are formed during the calcination of Ni foam loaded with Mg powders, which is evident in the examination of the Mg–Ni phase diagram [21]. Pure Ni remains at the core of the Ni foam struts after calcination at 600 °C for 30 min. The Mg_2Ni on the outer layer of the Ni foam struts are reconfirmed by the appearance of cracks in the outer layer of the Mg-alloyed Ni foam after alkaline BH_4^- solution treatment (the similar situation is shown in Fig. 4).

Fluorine treatment is a convenient method for enriching Ni on the surface layer of a Mg–Ni alloy [22]. The Mg-alloyed Ni foam was treated by a dilute HF solution (0.06 mol L^{-1}) for 60 min at 30 °C, and a layer of fluorine compound is formed on the Ni foam struts (Fig. 6). HF-treated Mg-alloyed Ni foams show higher specific surface areas than Mg-alloyed Ni foams (Table 1).

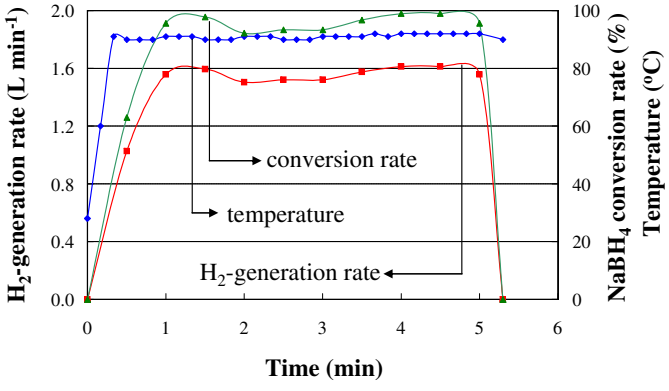

Fig. 10. H_2-generation rate and reaction plate temperature during falling film process. Raney-Ni foam 100 × 30 × 1.7 mm, 2.5 g. Fuel and feed rate: 15 wt.% of $NaBH_4$ + 10 wt.% of NaOH, at 4 mL min^{-1}.

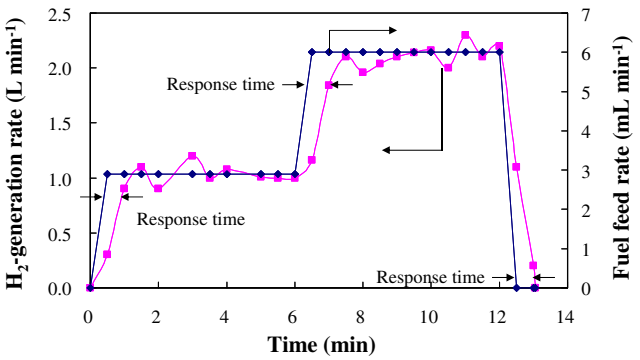

Fig. 11. Response of H_2-generation rate to fuel feed rate in falling film reactor. Reaction plate: Raney-Ni foam 100 × 30 × 1.7 mm, 2.5 g. Fuel and feed rate: 15 wt.% of $NaBH_4$ + 10 wt.% of NaOH, at 3 and 6 mL min^{-1}, respectively.

Fig. 7 shows the morphological change of the Al-alloyed Ni foam after the alkaline BH_4^- solution treatment. An examination of the Al–Ni binary equilibrium phase diagram [23] predicts that Al_3Ni (orthorhombic lattice) is a major phase that coexists with a minor phase Al_3Ni_2 (hexagonal lattice) [Fig. 8(c)]. Al in Al-alloyed Ni foam reacts with OH^- to generate H_2 during the alkaline BH_4^- solution treatment. H_2 bubbles, together with the H_2 generated from BH_4^- hydrolysis, remove loosely formed materials on Ni foam struts. A comparison of Fig. 8(b) and (d) shows a significantly widened Ni diffraction peak, which reveals that markedly fine Ni grains existed. A layer of Raney Ni was created on the Ni foam struts, and Raney Ni foam was formed by correlating the XRD and SEM results (Figs. 7 and 8).

3.2. H_2 generation

$NaBH_4$ generates a large amount of H_2 through the catalyzed hydrolysis reaction:

$$NaBH_4 + 2H_2O = NaBO_2 + 4H_2 + 300\ kJ \quad (1)$$

H_2 generation from BH_4^- hydrolysis catalyzed by bare Ni and surface-alloyed Ni foams is shown in Fig. 9. Surface-alloyed Ni foams significantly accelerate the BH_4^- hydrolysis reaction, thus revealing that catalytic sites are created by the surface alloying of Ni foam and subsequent treatments. On the basis of the physical characterization of the aforementioned catalysts and previous results [10,11], we observed that Mg_2Ni and Raney Ni existing on Ni foam struts behave as catalytic sites. Mg is a poor catalyst for BH_4^- hydrolysis reaction because $Mg(OH)_2$ is formed once Mg establishes contact with water, and BH_4^- is unable to reduce $Mg(OH)_2$. Ni serves as the best catalytic site on Mg-alloyed Ni foam struts. HF-treated Mg-alloyed Ni foam exhibits higher catalytic activities than Mg-alloyed Ni foams because Mg_2Ni is disproportionate to Ni and MgF_2 at the extreme surface during HF treatment [22].

In contrast to Mg-alloyed Ni foam, Al-alloyed Ni foam leaves Raney Ni on Ni foam struts after treatment with an alkaline BH_4^- solution (Figs. 7 and 8). BH_4^- directly establishes contact with Ni during BH_4^- hydrolysis when using Raney Ni foam as the catalyst. The created MgF_2 hinders the diffusion of BH_4^- to Ni in the HF-treated Mg-alloyed Ni foam. By contrast, Raney Ni foam has a higher specific surface area than Mg-alloyed Ni and HF-treated Mg-alloyed Ni foams (Table 1). Therefore, Raney Ni foam has the highest activity than the other foams (Fig. 9).

3.3. Falling film H_2 generation

Fig. 10 shows the H_2 generation rate and reaction plate temperature during falling film H_2 generation. The test apparatus (Fig. 2) rapidly establishes a stable H_2 generation within 1 min, whereas the reaction plate temperature is sustained at 90 °C. A high $NaBH_4$ conversion rate (more than 90%) indicates that only an insignificant amount of alkaline $NaBH_4$ solution has not come in contact with the reaction plate during the falling film process at a certain fuel feed rate. Fig. 11 shows the response of the H_2 generation rate to fuel feed rate. The H_2 generation rate increases and decreases with increasing and decreasing fuel feed rates, respectively. Stable H_2 generation is realized when fuel is supplied at a constant rate. H_2 generation catalyzed by Raney Ni foam quickly responds to fuel supply (less than 1 min as marked in Fig. 11).

An increase in fuel feed rate increases H_2 generation rate (Fig. 12). Raney Ni foam as the reaction plate exhibits a conversion rate dependent on the Raney Ni foam length (corresponding to residence time) with changing fuel feed rates. A comparison of Fig. 12(a) and (b) shows that the use of a BH_4^- solution with low $NaBH_4$ concentration decreases the dependence of conversion rate on Raney Ni foam length. Thus, a low $NaBH_4$ concentration in alkaline BH_4^- solution with less residence time is better than a high $NaBH_4$ concentration in the falling film process. An alkaline BH_4^- solution with high $NaBH_4$ concentration exhibits high H_2 generation rate but low $NaBH_4$ conversion rate when fuel is supplied at a constant rate. Detailed investigations on H_2 generation rates, $NaBH_4$ conversion rates, $NaBH_4$ concentrations, and residence

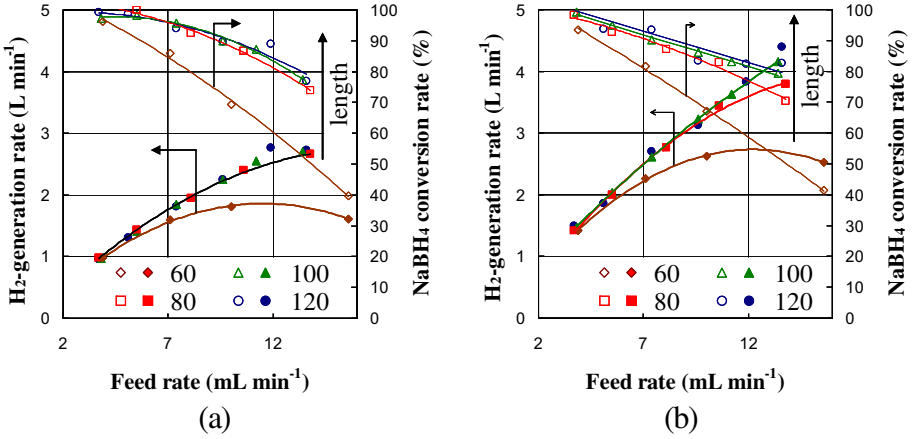

Fig. 12. Dependence of H_2-generation rate on fuel feed rate when using Raney Ni foam sheet with varied length from 60 to 120 mm in falling film reactor. The width and thickness are 30 and 1.7 mm, respectively. Fuel contains (a) 10 and (b) 15 wt.% of $NaBH_4$ in alkaline solution (10 wt.% of NaOH).

time reductions are necessary to develop an effective falling film reactor for H_2 generation from BH_4^- hydrolysis.

4. Conclusions

A new catalyst is developed to catalyze BH_4^- hydrolysis reaction based on surface alloying in Ni foam. Mg–Ni and Al–Ni intermetallic compounds are formed when heating Ni foam loaded with Mg and Al powders to 600 °C. The catalytic sites of Mg_2Ni and Raney Ni are created on Ni foam struts after the treatment of Mg- and Al-alloyed Ni foams with alkaline BH_4^- solution, respectively. Raney Ni on Ni foam struts (Raney Ni foam) has higher catalytic activity than Mg_2Ni on Ni foam struts. Raney Ni foam reaction plate in falling film reactor demonstrates high catalytic activity and quick response to fuel feed in H_2 generation.

Acknowledgments

This work is financially supported by the National Natural Science Foundation of China, Grant Nos. 20976156, 50971114, 21276229 and 51271164; the Zhejiang Provincial Natural Science Foundation of China, Grant No. Z4110126; and the Doctoral Fund from the Education Ministry of China (20100101110042).

References

[1] M. Yadav, Q. Xu, Energy Environ. Sci. 5 (2012) 9698–9725.
[2] J.H. Wee, K.Y. Lee, S.H. Kim, Fuel Process. Technol. 87 (2006) 811–819.
[3] Jung-Ho Wee, J. Power Sources 155 (2) (2006) 329–339.
[4] K. Kim, T. Kim, K. Lee, S. Kwon, J. Power Sources 196 (2011) 9069–9075.
[5] B.H. Liu, Z.P. Li, J. Power Sources 187 (2009) 527–534.
[6] Y. Shang, R. Chen, Energy Fuels 20 (2006) 2142–2148.
[7] Rajasree Retnamma, Augusto Q. Novais, C.M. Rangel, Int. J. Hydrogen Energy 36 (2011) 9772–9790.
[8] H.I. Schlesinger, H.C. Brown, A.B. Finholt, J.R. Gilbreath, H.R. Hockstra, E.K. Hydo, J. Am. Chem. Soc. 75 (1953) 215–219.
[9] H. Dong, H. Yang, X. Ai, C. Cha, Int. J. Hydrogen Energy 28 (2003) 1095–1100.
[10] B.H. Liu, Z.P. Li, S. Suda, J. Alloys Compd. 415 (2006) 288–293.
[11] S.C. Amendola, S.L. Sharp-Goldman, M.S. Janjua, M.T. Kelly, P.J. Petillo, M. Binder, J. Power Sources 85 (2000) 186–189.
[12] W. Ye, H. Zhang, D. Xu, L. Ma, B. Yi, J. Power Sources 164 (2007) 544–548.
[13] U.B. Demirci, F. Garin, J. Alloys Compd. 463 (2008) 107–111.
[14] U.B. Demirci, F. Garin, J. Mol. Catal. A Chem. 279 (1) (2008) 57–62.
[15] U.B. Demirci, F. Garin, Catal. Commun. 9 (2008) 1167–1172.
[16] Y. Chen, H. Kim, Mater. Lett. 62 (2008) 1451–1454.
[17] J. Lee, K.Y. Kong, C.R. Jung, E. Cho, S.P. Yoon, J. Han, T.G. Lee, S.W. Nam, Catal. Today 120 (2007) 305–310.
[18] H.B. Dai, Y. Liang, P. Wang, H.M. Cheng, J. Power Sources 177 (2008) 17–23.
[19] S. Suda, Y.-M. Sun, B.-H. Liu, Y. Zhou, S. Morimitsu, K. Arai, N. Tsukamoto, M. Uchida, Y. Candra, Z.-P. Li, J. Appl. Phys. A 72 (2001) 209–212.
[20] Z.P. Li, B.H. Liu, F.F. Liu, D. Xu, J. Power Sources 196 (2011) 3863–3867.
[21] Mohammad Mezbahul-Islam, Mamoun Medraj, CALPHAD Comput. Coupling Phase Diagrams Thermochem. 33 (3) (2009) 478–486.
[22] X.-L. Wang, N. Haraikawa, S. Suda, J. Alloys Compd. 231 (1995) 397.
[23] M. Hansen, A. Anderko, Constitution of Binary Alloys, McGraw-Hill, New York, 1958.